

# Analysis of Derivatized Wall Teichoic Acids Confirms that a Mutation in Phage-Resistant *Listeria monocytogenes* Impacts Rhamnose Decoration

Danielle M. Trudelle, Daniel W. Bryan, Shahla Ray, John P. Munafo, Jr.,\* and Thomas G. Denes\*



Cite This: *ACS Omega* 2022, 7, 17002–17013



Read Online

ACCESS |



Metrics & More

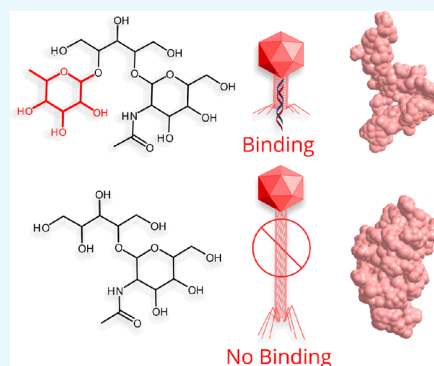


Article Recommendations



Supporting Information

**ABSTRACT:** *Listeria monocytogenes* is a Gram-positive foodborne pathogen that causes listeriosis, an illness that may result in serious health consequences or death. Wall teichoic acids (WTAs) are external cell wall glycopolymers that play many biological roles. Here, the WTA composition was determined for several phage-resistant mutant strains of *L. monocytogenes*. The strains included wild-type (WT) *L. monocytogenes* 10403S, and three phage-resistant mutant strains derived from 10403S, consisting of two well-characterized strains and one with unknown impact on cell physiology. Several WTA monomers were prepared from WT 10403S, as analytical standards. The WTA monomer fraction was then isolated from the mutant strains and the corresponding per-trimethylsilylated derivatives were analyzed by gas chromatography-flame ionization detection. WTA monomer, GlcNAc-Rha-Rbo, was detected in 10403S, and not detected in the phage-resistant strains known to lack rhamnose and *N*-acetylglucosamine; although the expected monomers GlcNAc-Rbo and Rha-Rbo were detected, respectively. GlcNAc-Rha-Rbo was also detected in strain UTK P1-0001, which is known to impact phage adsorption through an undetermined mechanism, albeit at a lower intensity than the WT 10403S, which is consistent with partial loss of function through truncation in RmlC protein. WTA monomers were also detected in an unpurified cell pellet, demonstrating that the method employed in this study can be used to rapidly screen *L. monocytogenes* without laborious WTA purification. This study lays the groundwork for future studies on WTA compositional analysis to support genomic data, and serves as a foundation for the development of new rapid methods for WTA compositional analysis.



## INTRODUCTION

*Listeria monocytogenes* is a foodborne pathogen that is known for its potential to cause listeriosis, a disease that may lead to serious illness or death in the young, old, immunocompromised, or pregnant.<sup>1</sup> Major outbreaks caused by listeriosis have been associated with various ready-to-eat (RTE) foods, including dairy products, produce, and deli meats.<sup>2–4</sup> Listeriosis currently ranks as one of the most deadly and costly foodborne illnesses in the U.S.<sup>5–7</sup> *L. monocytogenes* is a Gram-positive bacterium, indicated by the thick peptidoglycan (PG) layer comprising approximately 30–40% of its cell wall.<sup>8</sup> This substantial layer of PG supports the presence of glycopolymers (CWGs), which are attached either to the PG itself or to the cell membrane. In *Listeria*, CWG attached to the cell membrane are lipoteichoic acids (LTAs), while CWGs attached to the PG are wall teichoic acids (WTAs).<sup>9</sup> LTA and WTA share some important functions in the cell, including supporting cell division and morphology, biofilm formation, ion regulation, and virulence.<sup>10,11</sup> Although *Listeria* can survive without teichoic acids, or even a cell wall as L-form bacteria, such cells require specific growth conditions to do so, and lose functions associated with the cell wall and CWG.<sup>12</sup>

Unlike LTA, *Listeria* WTA display considerable variation within their glycosylation units, acting as the O-antigens for the cell, and are major determinants of the different serotypes (STs).<sup>13–15</sup> *L. monocytogenes* consists of at least 13 different ST, including 1/2a, 1/2b, 1/2c, 3a, 3b, 3c, 4a, 4b, 4ab, 4c, 4d, 4e and 7.<sup>16</sup> In this study, we focus on the model serotype 1/2a strain 10403S and its mutant derivatives. Over a ten year span, serotype 1/2a strains were responsible for approximately 40% of *L. monocytogenes* outbreaks in the U.S.<sup>17</sup> The ST 1/2, 3, and 7 strains display a type I WTA structure, consisting of a ribitol (Rbo) backbone with either *N*-acetylglucosamine (GlcNAc), rhamnose (Rha), or a hydroxyl group (OH) bound to carbons 2 and/or 4. Specifically, the 1/2 ST has a GlcNAc substituent at C2 and a Rha substituent at C4.<sup>15</sup> ST 3 WTA units are affected by a mutation in at least one of the genes necessary for WTA rhamnosylation, and therefore are lacking Rha in this

Received: December 31, 2021

Accepted: April 26, 2022

Published: May 11, 2022



Table 1. *L. monocytogenes* Strains and Features

<i>L. monocytogenes</i> Strain	Features	Reference
Wild-type Laboratory Strain		
10403S	Lineage II; 1/2a serotype (GlcNAc and Rha in WTA)	2
Mutant Strains		
FSL D4-0014	10403S mutant; nonsense mutation in <i>LMRG_00541</i> ; deficiency of GlcNAc in WTA; susceptible to phage LP-048 and resistant to LP-125 <sup>a</sup>	22
FSL D4-0119	10403S mutant; nonsense mutation in <i>LMRG_00542</i> ; deficiency of Rha in WTA; resistant to phages LP-048 and LP-125 <sup>a</sup>	22
UTK P1-0001	10403S mutant; frameshift mutation caused by a deletion in <i>LMRG_00544</i> ; truncated RmlC protein; susceptible to phage LP-125 and resistant to LP-048 <sup>a</sup>	23

<sup>a</sup>Resistance shown to occur through mechanism of adsorption inhibition.

structure.<sup>15</sup> ST 7 strains lack GlcNAc and Rha due to a mutation in at least one of the genes required for WTA rhamnosylation, as well as in at least one of the genes required for WTA *N*-acetylglucosaminylation.<sup>18</sup> Individual type I WTA units are bound at C1 and C5 of the Rbo by a phosphodiester linkage to form polymer chains approximately 21 units long.<sup>15,19</sup>

A pivotal role of WTA is that they serve as the receptors for bacteriophages (or “phages”), viruses that exclusively infect bacteria.<sup>9,20</sup> To replicate, phages inject genetic material into the bacterial host, where the cellular machinery of the host is utilized to produce progeny phage. At the end of this process, the host cell lyses from within, releasing the progeny phage into the environment.<sup>20</sup> A common form of bacterial resistance to *Listeria* phage infection occurs when the bacteriophages are unable to adsorb to their host. This process has been shown to occur through accumulation of mutations in genes impacting WTA glycosylation; in *L. monocytogenes* ST 1/2a strains, mutations that affect WTA rhamnosylation or *N*-acetylglucosaminylation significantly reduce the ability of bacteriophages to adsorb and infect.<sup>18,21,22</sup> Further, mutations causing loss of Rha in WTAs resist infection from almost all *Listeria* phages tested against it,<sup>23</sup> with only one characterized wild-type phage exception;<sup>24</sup> although phages were able to gain the ability to infect this type of resistant mutant through the process of *in vitro* evolution.<sup>25</sup> As phages are used as biocontrols in the food industry,<sup>26</sup> improving our knowledge of how *L. monocytogenes* can resist phage infection is critical for the long-term success of phage-based food safety applications.<sup>27</sup>

The structures of *Listeria* WTA have been analyzed using an array of different analytical methodologies. For the analysis of WTA structural components, methods including gel filtration chromatography,<sup>28,29</sup> permethylation combined with gas chromatography<sup>29,30</sup> with flame ionization detection<sup>31</sup> or mass spectrometry (MS)<sup>19</sup> have been previously reported. For analysis of molecular connectivity within the WTA structure, Smith degradation as well as general oxidation and reduction reactions have been used,<sup>28,29,32</sup> and nuclear magnetic resonance (NMR) spectra have been produced to determine anomeric configurations within the structure of the WTA.<sup>15,19,28,32</sup> More recently, major advances in WTA have been reported, including the employment of ultraperformance liquid chromatography (UPLC) with electrospray ionization (ESI) and tandem MS (MS/MS),<sup>15</sup> and ESI-MS/MS alone.<sup>33</sup> Although the methods used to determine WTA structures have progressively advanced over recent decades, unfortunately, there has not been a significant reduction in the time to obtain pure isolated WTA monomers used in the analysis. The current methods require extraction, purification, and hydrolysis of the WTA polymer before the sample can be analyzed.

Although the analysis of the pure WTA is fast employing UPLC-ESI-MS/MS, the instrumentation is not as common in commercial laboratories as gas chromatography-flame ionization detection (GC-FID), nor are WTA monomer reference materials commercially available. The published methods to isolate and purify WTA monomers are time-consuming and laborious. Accordingly, it would be helpful to develop methods with rapid sample preparation that employ common analytical instrumentation; however, pure WTA reference materials, which are currently lacking, are needed for using this approach.

The primary goal of this present investigation was to screen several phage-resistant mutant strains of *L. monocytogenes* for the presence of specific WTA monomers (Table 1; Figure 1)

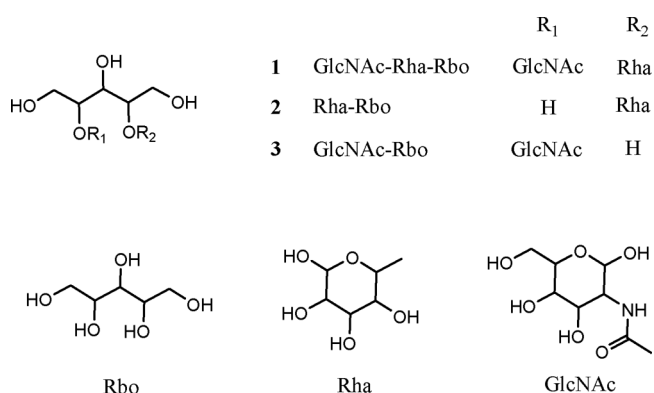
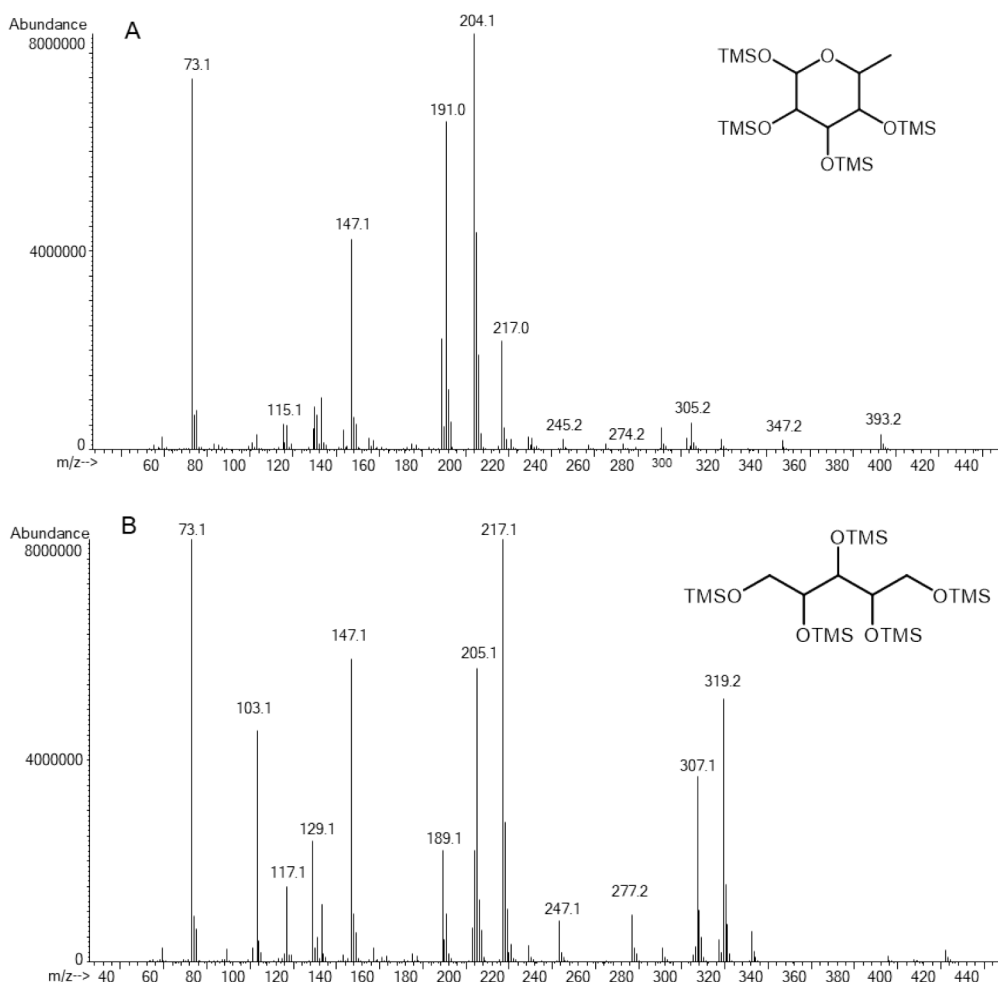


Figure 1. Chemical structures of (1) GlcNAc-Rha-Rbo, (2) Rha-Rbo, and (3) GlcNAc-Rbo.

using per-trimethylsilyl derivatization of the samples and employing gas chromatography - flame ionization detection (GC-FID). Two of the phage-resistant mutants, FSL D4-0014 and FSL D4-0119, have been well-characterized with known impact on WTA's and were included in the study as controls.<sup>22</sup> The third phage-resistant mutant, UTK P1-0001, has been genetically characterized. This genetic analysis suggested that the strain would express a truncated RmlC protein, which is known to impact rhamnosylation of WTA's; however, the strain shows a unique resistance pattern to phages through a mechanism of adsorption inhibition, and the impact of the mutation on WTA composition is unknown.<sup>23</sup> Accordingly, the three specific objectives of the present study were to (1) isolate WTA monomers as analytical standards; (2) analyze four different strains of *L. monocytogenes* by GC-FID, including (i) wild-type 10403S, (ii) phage-resistant mutant strain FSL D4-0119 (lacking Rha), (iii) phage-resistant mutant strain FSL D4-0014 (lacking GlcNAc), and (iv) phage-resistant mutant strain (UTK P1-0001), which possesses a truncated RmlC



**Figure 2.** EI mass spectrum of trimethylsilyl derivatives of (A) Rbo and (B) Rha, depicting the characteristic fragmentation pattern.

protein causing an undetermined impact on cell physiology; and (3) probe the feasibility of using the GC-FID method for WTA analysis of a single colony of *L. monocytogenes*.

## RESULTS AND DISCUSSION

**Preparation of WTA Analytical Standards.** The objective of this study was to screen several phage-resistant mutant strains of *L. monocytogenes* for their WTA composition using GC-FID. To accomplish this goal, first, the WTA monomer, GlcNAc-Rha-Rbo, was purified (Figure 1). Then the sample was further hydrolyzed, yielding a mixture of GlcNAc-Rha-Rbo, GlcNAc-Rha, and Rha-Rbo as a mixed analytical standard (Figure 1). GC-FID analysis of Rbo-5TMS in partial hydrolysates was used to determine a comparable degree of hydrolysis in the samples (Figure 2).

A mixture of GlcNAc-Rha-Rbo, GlcNAc-Rha, and Rha-Rbo was then per-trimethylsilylated, yielding GlcNAc-Rha-Rbo-9TMS, GlcNAc-Rbo-7TMS, and Rha-Rbo-7TMS, respectively (Figure 3), for GC-MS and GC-FID analysis. For comparison of WTA monomers in each sample, the areas of each WTA monomer were normalized based on the area of Rbo-5TMS in the 10403S sample (Figure 4).

The preparation of the WTA reference material from 10403S proceeded as follows. The yields denoted after each purification step were calculated from the prior step. *L. monocytogenes*, wild-type 10403S, was grown on brain heart infusion (BHI) media (5 L) to a density of 0.8–0.9 OD<sub>600</sub>.

The cells were harvested and autoclaved yielding the autoclaved cell pellet (ACP) (17.5 g). The ACP was then mechanically lysed, yielding isolated cell wall material (CWM) (8.5 g, 47.7% yield). The CWM was then subjected to enzyme treatment and washed, yielding the cell wall carbohydrate fraction (CWCF) (160 mg, 1.9% yield). The CWCF was then hydrolyzed and dialyzed, yielding the crude WTA polymer (cWTA polymer) (39 mg, 24.4% yield). The cWTA polymer was then further purified by anion-exchange chromatography, yielding purified WTA polymer (pWTA polymer) (3 mg, 7.69% yield). The pWTA polymer was then subjected to hydrolysis, using hydrogen fluoride (HF), and lyophilized, yielding purified WTA monomer, GlcNAc-Rha-Rbo (1 mg, 33.3% yield). The purity of GlcNAc-Rha-Rbo was >98%, as confirmed by liquid chromatography-mass spectrometry (LC-MS), high resolution electrospray ionization–time-of-flight mass spectrometry (HRESI-TOFMS), GC-FID, and GC-MS. After the initial isolation of GlcNAc-Rha-Rbo, the material was further partially hydrolyzed. The acid-catalyzed hydrolysis was monitored by GC-MS, and finally yielded a mixture of GlcNAc-Rha-Rbo, GlcNAc-Rha, and Rha-Rbo.

**Analytical Confirmation of WTA Analytical Standards.** The WTA monomers were subjected to LC-MS, HRESI-TOFMS, GC-FID, and GC-MS for structural confirmation. For GlcNAc-Rha-Rbo, a single peak was observed by LC-MS analysis, and upon TMS derivatization and GC-FID and GC-MS analysis, a single chromatographic peak was also observed.

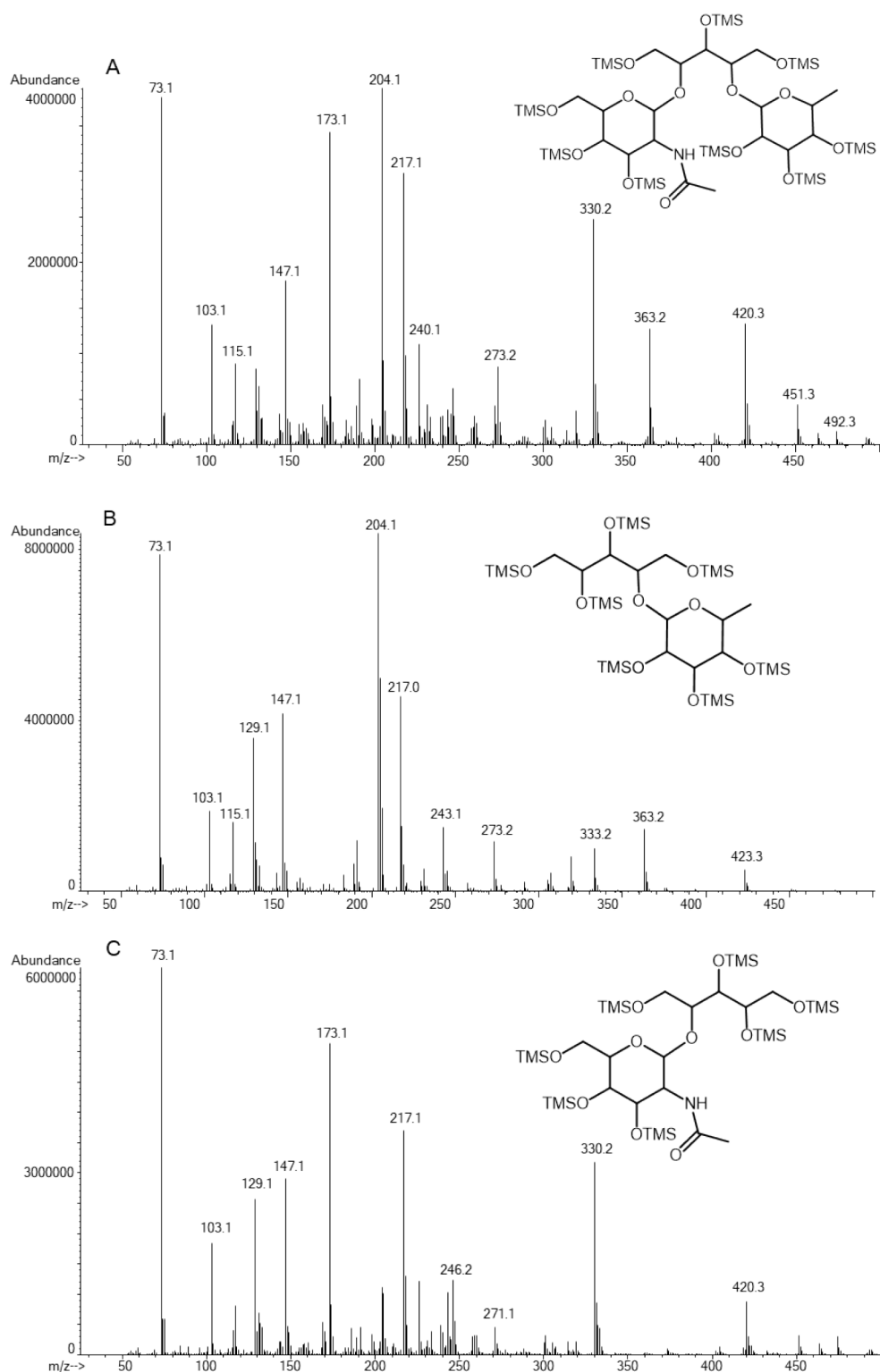


**Figure 3.** EI mass spectrum of trimethylsilyl derivatives of (A) GlcNAc-Rha-Rbo, (B) Rha-Rbo, and (C) GlcNAc-Rbo, depicting the characteristic fragmentation pattern.

Upon LC-MS analysis, a base ion at  $m/z$  500.2 (100,  $[M - H]^-$ ) and an ion at  $m/z$  1001.5 (18,  $[2M - H]^-$ ) was observed, both consistent with a molecular weight of 501.2 Da. Upon HRESI-TOFMS analysis, a sodium adduct at  $[M + Na]^+$   $m/z$  524.1949 was observed (calculated for  $NaC_{19}H_{35}NO_{14}$ ,  $m/z$  524.1950). These results are consistent with the analytical data for the purified GlcNAc-Rha-Rbo, previously reported as

the WTA monomer unit of a ST 1/2a strain of *L. monocytogenes*.<sup>33</sup> The EI-MS spectrum of the per-trimethylsilylated derivative of GlcNAc-Rha-Rbo, GlcNAc-Rha-Rbo-9TMS, was also in agreement with GlcNAc-Rha-Rbo (Figure 3). The retention index (RI) for GlcNAc-Rha-Rbo-9TMS on a DB-5 column was calculated as  $RI = 3515$ .

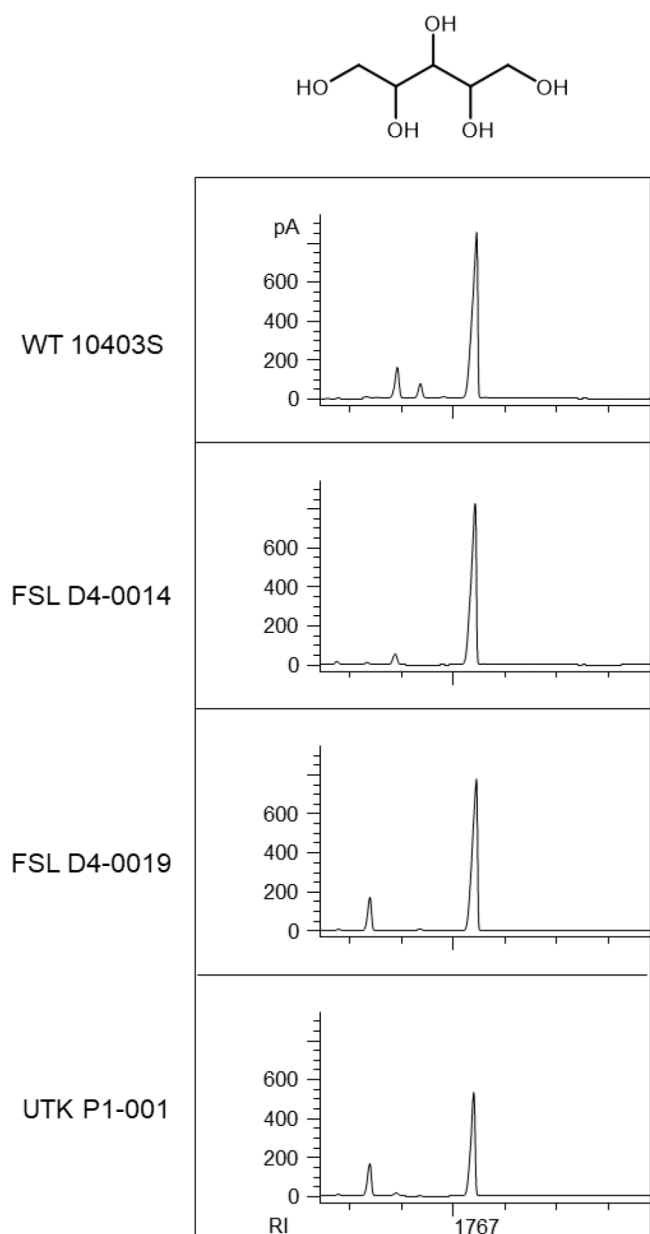


**Figure 4.** GC-FID analysis of Rbo-5TMS in partial hydrolysate of 10403S, FSL D4-0119, FSL D4-0014, and UTK P1-0001 WTA fractions. GC-FID analysis of Rbo-5TMS in partial hydrolysates was used to determine a comparable degree of hydrolysis in the samples.

After initial isolation, the material was further hydrolyzed yielding a mixture of GlcNAc-Rha-Rbo, GlcNAc-Rha, and Rha-Rbo. Accordingly, the WTA mixture was employed as a reference material to generate RIs of the per-trimethylsilylated derivatives of the WTAs for GC-FID method development. Upon LC-MS analysis of Rha-Rbo, a base ion at  $m/z$  321.1 [100, M + Na]<sup>+</sup> and an ion at  $m/z$  298.1 [100, M – H]<sup>–</sup> was observed, both consistent with a molecular weight of 298.3 Da. Upon HRESI-TOFMS analysis of Rha-Rbo, a sodium adduct at [M + Na]<sup>+</sup>  $m/z$  321.1150 was observed (calculated for NaC<sub>11</sub>H<sub>22</sub>O<sub>9</sub>,  $m/z$  321.1156). The EI-MS spectrum of the per-trimethylsilylated derivative of Rha-Rbo, Rha-Rbo-7TMS, was also in agreement with Rha-Rbo (Figure 3). The RI for Rha-Rbo-7TMS on a DB-5 column was calculated as RI = 2487.

Upon LC-MS analysis of GlcNAc-Rbo, a base ion at  $m/z$  378.1 [100, M + Na]<sup>+</sup> and an ion at  $m/z$  354.1 [100, M – H]<sup>–</sup> was observed, both consistent with a molecular weight of 355.3 Da. Upon HRESI-TOFMS analysis of GlcNAc-Rbo, a sodium adduct at [M + Na]<sup>+</sup>  $m/z$  378.1376 was observed (calculated for NaC<sub>13</sub>H<sub>25</sub>NO<sub>10</sub>,  $m/z$  378.1370). The EI-MS spectrum of the per-trimethylsilylated derivative of GlcNAc-Rbo, GlcNAc-Rbo-7TMS, was also in agreement with GlcNAc-Rbo (Figure 3). The RI for GlcNAc-Rbo-7TMS on a DB-5 column was calculated as RI = 2845. The results from these experiments allowed for the development of a GC-FID method to separate all three of the derivatized WTAs with good chromatographic resolution.

**Analysis of WTA Monomers in *L. monocytogenes* Serotype 1/2a Mutants.** GC-FID was employed to confirm the presence or absence of wall teichoic acid monomers, including the complete GlcNAc-Rha-Rbo or partial GlcNAc-Rbo and Rha-Rbo variants, in the following strains: (1) *L. monocytogenes* wild-type strain 10403S (Rha<sup>+</sup>, GlcNAc<sup>+</sup>), (2) mutant strain FSL D4-0014 (Rha<sup>+</sup>, GlcNAc<sup>–</sup>), (3) mutant strain FSL D4-0119 (Rha<sup>–</sup>, GlcNAc<sup>+</sup>), and (4) mutant strain UTK P1-0001 (truncated RmlC protein). As anticipated, GlcNAc-Rha-Rbo was detected in wild-type strain 10403S as the GlcNAc-Rha-Rbo-9TMS derivative. Also, GlcNAc-Rha-Rbo was detected in UTK P1-0001 (truncated RmlC protein), albeit at levels ~11% those of 10403S (Figure 5). In addition, Rha-4TMS and Rha-Rbo-7TMS were detected in both strains; however, Rha and Rha-Rbo were also present at lower levels in the UTK P1-0001 strain (~13% and ~11% those of 10403S, respectively). UTK P1-0001 was previously found to have a mutation in a gene coding for RmlC,<sup>23</sup> an epimerase that is involved in the biosynthesis of Rha.<sup>34</sup> This mutation was shown to cause a premature stop codon in the *rmlC* gene that would only result in the loss of the last three amino acids of RmlC, therefore its function is unlikely to be completely inhibited,<sup>23</sup> which is consistent with our observations of less observed Rha in the strain. Additionally, this strain has previously demonstrated binding to the *Listeria* phage LP-125, which requires both GlcNAc and Rha for adsorption.<sup>22,23</sup> The results from this study suggest that RmlC in UTK P1-0001 has reduced activity, resulting in less rhamnosylation of the WTA; this would explain the unusual phage resistance phenotype where LP-125 (requiring both GlcNAc and Rha for binding) is able to adsorb to the strain, whereas LP-048 (requiring only Rha) does not appear to efficiently adsorb.<sup>23</sup> Thus, LP-048 binding correlates with the observed reduction in WTA Rha composition in UTK P1-0001. Future studies should explore the potential for this type of mutation to impact biofilm formation, virulence, and resistance to antimicrobials, as rhamnose and other WTA structures have been implicated in these processes for *L. monocytogenes*.<sup>13,35–37</sup>

In the FSL D4-0014 (Rha<sup>+</sup>, GlcNAc<sup>–</sup>) mutant strain, GlcNAc-Rha-Rbo was not detected, which is consistent with previous results showing that FSL D4-0014 is deficient in GlcNAc, and therefore would be lacking GlcNAc-Rha-Rbo as a WTA monomer. In contrast, Rha-4TMS and Rha-Rbo-7TMS were detected in FSL D4-0014. FSL D4-0014 is a 10403S derived mutant, with a loss of function mutation in a glycosyltransferase gene, *lmo1079*, responsible for addition of GlcNAc in WTA.<sup>18,22</sup> Phage binding and wheat germ agglutination assays previously confirmed the expected result. In the FSL D4-0119 (Rha<sup>–</sup>, GlcNAc<sup>+</sup>) mutant strain, neither GlcNAc-Rha-Rbo nor Rha was detected; although GlcNAc-

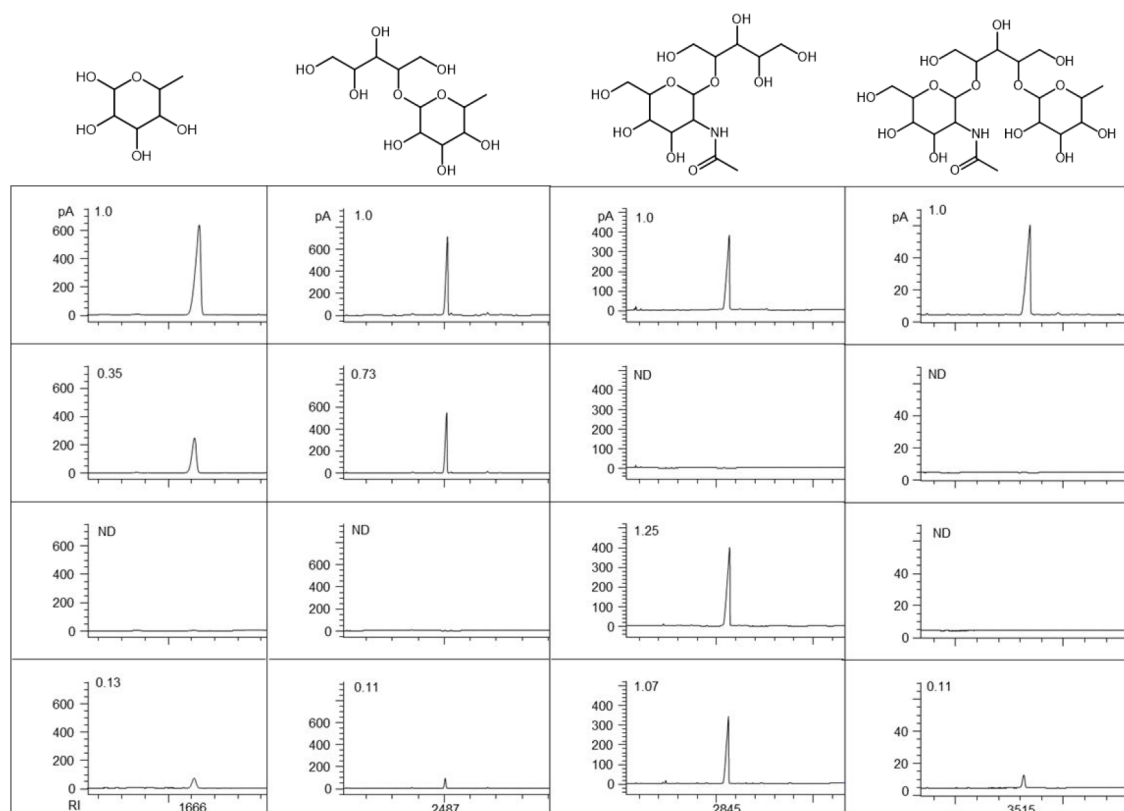


**Figure 5.** Comparison of Rha, Rha-Rbo, GlcNAc-Rbo, and GlcNAc-Rha-Rbo in the partial hydrolysate of 10403S, FSL D4-0119, FSL D4-0014, and UTK P1-0001 WTA fractions. All chromatographic peaks are per-trimethylsilylated derivatives analyzed by GC-FID. The factor denoted in the upper left corner of each trace was calculated by dividing the area of the analyte in the mutant sample by the area of the analyte in the 10403S sample. For comparison of WTA monomers in each mutant strain, the areas of each WTA monomer were normalized based on the area of Rbo-7TMS in the 10403S strain. ND; not detected.

Rbo was detected at levels  $\sim 25\%$  higher than in 10403S (Figure 5). FSL D4-0119 is a 10403S derived mutant with a loss of function mutation (nonsense mutation) in another glycosyltransferase, *lmo1080*, which is known to be required for rhamnosylation of WTA.<sup>18,22</sup> Consistent with the results, sequencing data and phage spot tests/adsorption assays demonstrated that FSL D4-0119 is deficient in Rha.<sup>22</sup>

On the basis of the genomic data, each one of the phage-resistant mutant strains have a mutation in a glycosyltransferase associated with WTA decoration. It has been shown that these genes are consistent hotspots for mutations conferring phage resistance.<sup>18,22,25</sup> In this present study, the WTA fraction of each of the mutant strains tested here was purified and analyzed by GC-FID, confirming the presence (UTK P1-0001; lower levels than 10403S) or absence (FSL D4-0014, FSL D4-0119; not detected) of GlcNAc-Rha-Rbo. This compositional data supports the genomic data and the approach used in this study may be employed as a tool to characterize different strains of *L. monocytogenes*. To develop high-throughput WTA compositional analysis, more rapid methods are needed to keep pace with the advancements in genomic data sets.

**Analysis of WTA Monomers in Less Processed Samples.** In the present study, GC-FID confirmation of the presence or absence of GlcNAc-Rha-Rbo, GlcNAc-Rha, and Rha-Rbo from the purified WTA monomer fraction of each *L. monocytogenes* strain was successful (Figure 5); however, the sample preparation for each strain was extensive. The sample preparation required the culture of large quantities of bacteria (5 L; each) and the purification was laborious, including

mechanical, chemical, and enzymatic, treatments coupled with chromatographic purification. To assess the feasibility of using the GC-FID method to identify GlcNAc-Rha-Rbo, GlcNAc-Rha, and Rha-Rbo using smaller quantities of bacteria with less processing, samples were collected at four steps throughout the WTA purification process using the wild-type 10403S strain. The four samples included, in decreasing purity, (1) purified GlcNAc-Rha-Rbo, (2) crude WTA polymer (cWTA polymer), (3) CWCF (cell wall carbohydrate fraction), and (4) ACP (autoclaved cell pellet). The three in-process samples, cWTA polymer, CWCF, and ACP were subjected to HF hydrolysis prior to derivatization. All samples, were derivatized with *N,O*-bis(trimethylsilyl)trifluoroacetamide (BSTFA) with 1% trimethylchlorosilane (TMCS) prior to GC-FID analysis.

Interestingly, GlcNAc-Rha-Rbo, GlcNAc-Rha, and Rha-Rbo were detected in all the in-process samples analyzed, including the ACP sample that were only steam-killed cells (Figure 6).

The calculated signal-to-noise ratio (SNR) for GlcNAc-Rbo-7TMS, Rha-Rbo-7TMS, and GlcNAc-Rha-Rbo-9TMS in the ACP sample was 923:1, 33:1, and 409:1, respectively (see the Supporting Information). The SNR for the per-trimethylsilylated WTA components using the current unoptimized method ranged from 11 to 309 times greater than the standard 3:1 value for the limit of detection (LOD) and 3 to 41 times greater than the standard 10:1 value for the limit of quantification (LOQ). The results of this experiment suggest that the analytical method may be further optimized to serve as a faster and less expensive alternative to the currently published analytical methods for WTA detection and

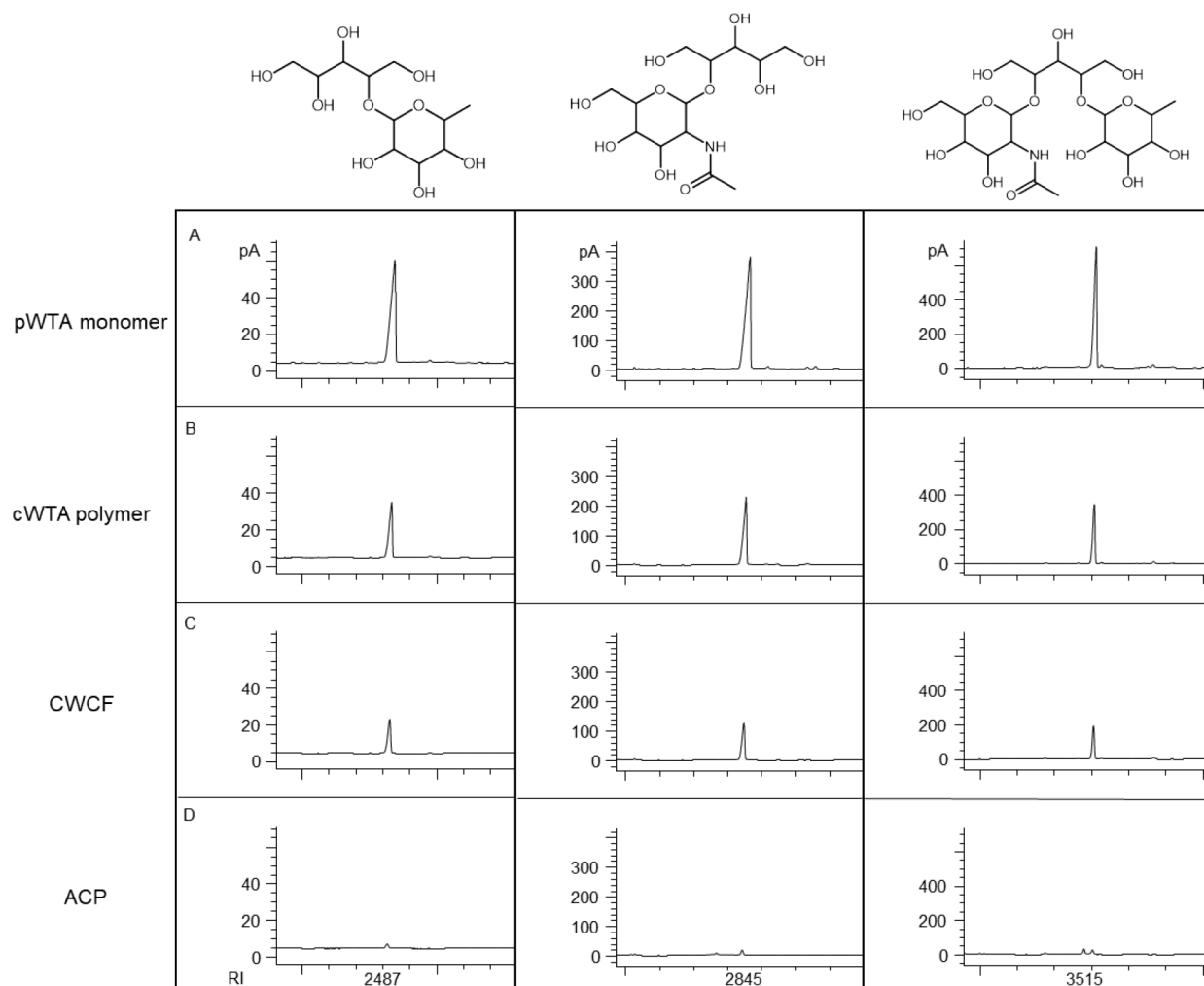


**Figure 6.** Streamlining sample preparation for rapid analysis of trimethylsilyl derivatives of WTA monomers by GC-FID. (A) Purified WTA monomer (pWTA monomer), (B) crude WTA polymer (cWTA polymer), (C) CWCF, and (D) ACP. The strain used was 10403S.

quantitation. Derivatization and GC-FID analysis of ACP samples require significantly less sample, time, reagents, and equipment than purifying WTA samples and analysis by UPLC-ESI-MS/MS.<sup>14</sup> We show that this method can reduce the volume of broth-grown culture of *L. monocytogenes* needed for analysis from several liters to several milliliters. In addition, the method eliminates time-consuming steps, costly reagents, and specialized equipment. Processing steps that are eliminated include lysing cells with a French Press, enzymatic treatment of the lysates, anion-exchange chromatography, and phosphate testing of eluent fractions, while still detecting WTA monomers above the standard LOQ. However, the limitation to the current method is that more analytical standards would need to be commercially available to develop the method for additional WTA monomers with variable composition. This approach would offer an analytical alternative to rapid protein-binding methods, such as Sumrall et al's use of phage-derived recombinant affinity proteins to glycotype *Listeria*.<sup>38</sup> Whereas protein-binding methods may be particularly useful for rapid indirect determination of exposed cell-surface physiology, the analytical methods described here would provide direct quantitative measures of specific WTA components. GC-FID analysis of per-trimethylsilylated derivatives of WTAs with different configurations may also be chromatographically resolved, including WTAs containing diastereomers such as

glucose and galactose, and enantiomers, if chiral capillary columns such as a 2,3-diacetoxy-6-*O*-*tert*-butyl dimethylsilyl  $\gamma$ -cyclodextrin (Rt- $\gamma$ DEXsa) or a 2,3-di-*O*-methyl-6-*O*-*tert*-butyl dimethylsilyl  $\beta$ -cyclodextrin (Rt- $\beta$ DEXsm) are employed; however, additional evaluations are needed to test these hypotheses. Furthermore, the results from the GC-FID analysis of the CWCF sample indicates there is little benefit in purifying the sample beyond enzymatic treatment of the cell lysate; by stopping here significant time and resources are saved, and the resulting peak intensity is still about 50% the intensity of the fully purified WTA sample. To develop a robust analytical method that can discriminate a collection of WTA acid monomers with differing carbohydrate moieties and structural configurations, more WTA reference materials would need to be available as analytical standards.

In conclusion, in this study, we used GC-FID, GC-MS, and LC-MS to confirm the composition of wall teichoic acids in phage-resistant mutants of *L. monocytogenes*. Interestingly, we show that the unique phage resistance phenotype observed in 10403S derived mutant UTK P1-0001 is likely due to a significantly diminished relative abundance of Rha decoration in the wall teichoic acids, indicating the relevance of partial loss of function mutations in phage-host interactions. Further, we show that the process of observing wall teichoic acid monomers can be significantly streamlined by analyzing

unpurified samples by GC-FID. Taken together, the work presented here provides a roadmap for the rapid characterization of *Listeria* WTA composition; this can provide valuable information on key aspects of *Listeria* biology such as determining phage susceptibility patterns, virulence potential, subtyping information, and basic cell physiology.

## MATERIALS AND METHODS

**Bacterial Growth Conditions.** Working stocks of *L. monocytogenes* strains (Table 1) were stored at  $-80\text{ }^{\circ}\text{C}$  in BHI (Becton Dickinson, Sparks, MD) broth with 15% (wt/vol) glycerol. *L. monocytogenes* was streaked onto 1.5% (wt/vol) BHI agar and then incubated at  $30\text{ }^{\circ}\text{C}$  for approximately 24 h. Erlenmeyer flasks (125 mL) containing 30 mL of BHI broth were used for overnight (ON) cultures and inoculated with three similar sized colonies from a streak plate stored at  $4\text{ }^{\circ}\text{C}$  for less than 2 weeks prior. The inoculated BHI broth was then incubated for 16 h at  $30\text{ }^{\circ}\text{C}$  shaking at 160 rpm. ON culture was added to Erlenmeyer flasks 1/4 full with sterile BHI broth in a 1:100 ratio (ON culture to BHI) and incubated at  $30\text{ }^{\circ}\text{C}$  shaking at 160 rpm. Cells were grown to an  $\text{OD}_{600}$  between approximately 0.8 and 1.0 (GENESYS 30 Visible Light Spectrophotometer; Thermo Scientific, Waltham, MA), then autoclaved for 30 min at  $121.1\text{ }^{\circ}\text{C}$ . Flasks were cooled to approximately  $4\text{ }^{\circ}\text{C}$  in an ice water bath, then the culture was aliquoted into centrifuge bottles and centrifuged (Beckman J2-HS; Beckman Coulter Life Sciences, Indianapolis, IN) at  $7000g$  for 10 min at  $4\text{ }^{\circ}\text{C}$  to pellet cells. The ACPs were collected and frozen for storage at  $-20\text{ }^{\circ}\text{C}$ .

**Chemicals and Reagents.** Anhydrous pyridine (reagent grade), BSTFA with 1% TMCS, formic acid, glycerol, glycine, HCl, methanol (HPLC grade), NaCl, NaOH, proteinase K, sodium dodecyl sulfate, Tris base, and hydrofluoric acid (48–51%) were purchased from Thermo Fisher Scientific (Waltham, MA). A mixture of *n*-alkanes C9–C18 was purchased from Phenomenex (Torrance, CA) and *n*-alkanes C19, C20, and a mixture of C21–C40 were purchased from Millipore Sigma (Burlington, MA). BHI was purchased from Becton Dickinson (Sparks, MD).  $\text{MgSO}_4$  was purchased from Acros Organics (Geel, Belgium). DNase and RNase were purchased from Alfa Aesar (Tewksbury, MA). A phosphate standard solution was purchased from Merck (Darmstadt, Germany).

**Purification of WTA Monomer Reference Materials.**  
**Cell Lysis.** Analytical standards of the WTAs (GlcNAc-Rha-Rbo, GlcNAc-Rha, and Rha-Rbo) were isolated following a previously reported procedure with some modifications.<sup>14</sup> The WTA monomers, GlcNAc-Rha and Rha-Rbo, were generated through acid catalyzed hydrolysis of GlcNAc-Rha-Rbo. Frozen cell pellets of *L. monocytogenes*, wild-type 10403S, previously reported to contain WTA monomer GlcNAc-Rha-Rbo were thawed to room temperature (RT) and resuspended in a saline magnesium (SM) buffer to a density of approximately 0.75 g cells/mL. Cells were lysed by at least two passages through a French Press Pressure Cell (French Press Cell Disrupter; Thermo Electron Corporation, Milford, MA) at 270 MPa. Lysed cells were centrifuged (Eppendorf 5804 R; Eppendorf, Hamburg, Germany) at  $1400g$  for 5 min to remove unbroken cells. The supernatant was collected and centrifuged (Beckman J2-HS; Beckman Coulter Life Sciences, Indianapolis, IN) at  $20,000g$  for 30 min at  $4\text{ }^{\circ}\text{C}$  to recover cell walls. Pellets were collected from the supernatant until no more visible solid material remained (9 collections total per strain) which were

then washed twice with sterile ultrapure water ( $20,000g$  for 30 min at  $4\text{ }^{\circ}\text{C}$ ). The CWM was pooled into Nalgene Oak Ridge tubes (Thermo Scientific, Waltham, MA), combined and frozen for storage at  $-20\text{ }^{\circ}\text{C}$ .

**Cell Wall Purification.** Frozen cell wall materials were thawed to RT, weighed, and resuspended in 10 mM Tris–Cl (pH 7.6) for a combined volume of  $36\,867\text{ }\mu\text{L}$ . The DNase (Alfa Aesar, Tewksbury, MA) working solution was prepared by mixing DNase powder (lyophilized by manufacturer in 2.5 mM calcium acetate and 2.5 mM magnesium sulfate) with sterile ultrapure water to a concentration of 10 mg/mL. The RNase (Alfa Aesar, Tewksbury, MA) working solution was prepared by mixing lyophilized RNase powder with 100 mM Tris–Cl (pH 7.6) to a concentration of 10 mg/mL. The proteinase K (Fisher Scientific, Fair Lawn, NJ) working solution was prepared by mixing lyophilized proteinase K powder with 10 mM Tris–Cl (pH 7.6) to a concentration of 10 mg/mL. Cell wall materials were mixed with DNase and RNase working solutions ( $376\text{ }\mu\text{L}$  each) together with each enzyme at a final concentration of  $100\text{ }\mu\text{g}/\text{mL}$ , then inverted 20 times and incubated at  $25\text{ }^{\circ}\text{C}$  for 3.5 h with two inversions. Following this,  $380\text{ }\mu\text{L}$  of the proteinase K working solution was added for a final concentration of  $100\text{ }\mu\text{g}/\text{mL}$ , inverted 20 times, and incubated at  $25\text{ }^{\circ}\text{C}$  for 2 h with inversions every 30 min. After enzyme treatments, cell walls were pelleted by centrifugation at  $20,000g$  for 30 min at  $4\text{ }^{\circ}\text{C}$  (Beckman J2-HS; Beckman Coulter Life Sciences, Indianapolis, IN). The supernatant was discarded, and pellets were stored overnight at  $4\text{ }^{\circ}\text{C}$ . Following this, pellets were resuspended with 30 mL of a 4% (w/v) sodium dodecyl sulfate (SDS) solution and aliquoted into glass tubes ( $\sim 10\text{--}12\text{ mL}$  per tube). Tubes were incubated in water for 30 min at  $100\text{ }^{\circ}\text{C}$ . After cooling to RT, sample aliquots were recombined into Nalgene Oak Ridge tubes and SDS-insoluble material (cell pellet) was collected by centrifugation at  $20,000g$  for 30 min at  $20\text{ }^{\circ}\text{C}$  (Beckman J2-HS; Beckman Coulter Life Sciences, Indianapolis, IN). Detergent was removed after washing the pellet five times with sterile ultrapure water at  $20,000g$  for 30 min at  $20\text{ }^{\circ}\text{C}$ . The resulting CWCF was then resuspended in 5 mL of sterile ultrapure water and transferred into 50 mL centrifuge tubes, frozen on an angle at  $-20\text{ }^{\circ}\text{C}$ , then lyophilized (VirTis Advantage Plus EL-85; SP Scientific, Gardiner, NY) and stored at  $-20\text{ }^{\circ}\text{C}$  with desiccant.

**Wall Teichoic Acid Extraction.** The lyophilized carbohydrate fraction of treated cells was mixed with 25 mM glycine/HCl buffer (pH 2.5) in Reacti-Vials (Thermo Fisher Scientific Inc., Waltham, MA) and hydrolyzed for 10 min at  $100\text{ }^{\circ}\text{C}$ . After cooling to RT, samples were centrifuged (Avanti J-26 XP; Beckman Coulter Life Sciences, Indianapolis, IN) at  $30,000g$  for 30 min at  $4\text{ }^{\circ}\text{C}$  to pellet insoluble materials. The supernatant was collected, and the pellet was resuspended in the same buffer. Hydrolysis and centrifugation were repeated twice; all collected supernatant was pooled and dialyzed (20 mL D-Tube Dialyzer Mega, MWCO 3.5 kDa; MilliporeSigma, Burlington, MA) at  $4\text{ }^{\circ}\text{C}$  against 2 L of ultrapure water for approximately 24 h (with one change of water at 12 h) to remove the buffer. The cWTA polymer solution was then frozen on a slant at  $-20\text{ }^{\circ}\text{C}$ , lyophilized, and stored at  $-20\text{ }^{\circ}\text{C}$  with a desiccant.

**Wall Teichoic Acid Polymer Purification.** The cWTA polymer (10 mg) was dissolved in a starting buffer ( $750\text{ }\mu\text{L}$  of 10 mM Tris–HCl, pH 7.5) and manually loaded onto the ÄKTA pure (GE Healthcare Bio-Sciences AB, Uppsala,

Sweden) LC system. WTA purification was performed with anion-exchange chromatography using a HiTrap DEAE FF Column (5 mL; GE Healthcare Bio-Sciences AB, Uppsala, Sweden). The column was first equilibrated with two column volumes of the starting buffer at a flow rate of 5 mL/min, then 20 column volumes of fractions were collected at a flow rate of 1 mL/min into tubes by elution using a linear gradient of 0–1 M NaCl solution. Starting and elution buffers were filtered through a 0.45  $\mu\text{m}$  Nylon membrane (Whatman-GE Healthcare, Buckinghamshire, United Kingdom) before use in the ÄKTA system. All glassware used for buffer preparation and storage was acid washed with a 10% HCl solution and rinsed with deionized (DI) and ultrapure water before use to prevent phosphate contamination.

**Phosphate Standard Curve Preparation.** A working stock solution of phosphate standard with a concentration of 10 mg/L  $\text{PO}_4$  was prepared from a phosphate standard solution (Merck, Darmstadt, Germany) with a concentration of 1000 mg/L  $\text{PO}_4$ . From the working stock solution, 5 mL phosphate standards were prepared in concentrations ranging from 0 to 5 mg/L  $\text{PO}_4$ . A phosphate test kit (Spectroquant; Merck, Darmstadt, Germany) was applied to each standard as well as an ultrapure water blank as per manufacturers' instructions. Absorbencies of each standard were read in 10 mm cuvettes with a spectrophotometer (GENESYS 30 Visible Spectrophotometer; Thermo Fisher Scientific, Madison, WI) at a wavelength of 690 nm. A standard curve was developed using Microsoft Excel (Version 1811) to establish a linear regression formula ( $y = 0.1613x + 0.0094$ ) for determining unknown phosphate values based on sample absorbencies at 690 nm.

**Determination of Wall Teichoic Acid Containing Fractions.** Fractions obtained after WTA purification were tested for UV activity using 1 mL samples aliquoted into acid-washed quartz cuvettes. Absorbance was read at a wavelength of 205 nm using the NanoDrop One Spectrophotometer (Thermo Fisher Scientific Inc., Waltham, MA) against a blank containing a 1:1 mixture of 10 mM Tris-HCl, pH 7.5 and 1 M NaCl. A 30  $\mu\text{L}$  subsample was taken from fractions showing absorbency at 205 nm, diluted to a total volume of 5 mL with ultrapure water, and treated with decomposition reagent (NANOCOLOR NanOx Metal; Macherey-Nagel, Düren, Germany) as per manufacturer's instructions. A blank of ultrapure water was treated the same way. A phosphate test kit (Spectroquant; Merck, Darmstadt, Germany) was then applied to the treated subsamples as well as the blank as per manufacturer's instructions. Absorbencies were read by spectrophotometry (GENESYS 30 Visible Light Spectrophotometer; Thermo Scientific, Waltham, MA) at a wavelength of 690 nm to calculate phosphate concentration using the formula obtained from the phosphate standard curve ( $y = 0.1613x + 0.0094$ ). Fractions calculated as having over 25 mg/L  $\text{PO}_4$  were dialyzed (20 mL D-Tube Dialyzer Mega, MWCO 3.5 kDa; MilliporeSigma, Burlington, MA) at 4  $^\circ\text{C}$  against 2 L ultrapure water for 24 h (with one change of water at 12 h) to remove the buffer. The pWTA polymer solution was then frozen on a slant at  $-20\text{ }^\circ\text{C}$ , lyophilized, and stored at  $-20\text{ }^\circ\text{C}$  with desiccant.

**Hydrofluoric Acid Hydrolysis.** Samples (2 mg; pWTA polymer) were subjected to hydrolysis using 200  $\mu\text{L}$  of HF (48–51%) at 0  $^\circ\text{C}$  for 24 h prior to evaporation over NaOH pellets in a chamber under vacuum. The reaction was monitored yielding the first intact GlcNAc-Rha-Rbo monomer.

Then the reaction was allowed to proceed for a longer time, yielding a mixture of GlcNAc-Rha and Rha-Rbo as partial hydrolysis products. Samples were subjected to a vacuum until HF evaporation was complete; the sample was then mixed with 500  $\mu\text{L}$  of ultrapure water, frozen at  $-20\text{ }^\circ\text{C}$ , lyophilized, and stored at  $-20\text{ }^\circ\text{C}$  with a desiccant. GC-FID analysis of Rbo-5TMS in partial hydrolysates was used to determine a comparable degree of hydrolysis in the samples.

**GlcNAc-Rha-Rbo.**  $\text{C}_{19}\text{H}_{35}\text{NO}_{14}$ ; HR-ToF-MS (ESI+)  $m/z$  524.1949 ( $[\text{M} + \text{Na}]^+$ , measured);  $m/z$  524.1950 ( $[\text{M} + \text{Na}]^+$ , calculated for  $\text{NaC}_{19}\text{H}_{35}\text{NO}_{14}$ ; ESI<sup>+</sup>-MS,  $m/z$  524.1  $[\text{100}, 2 \text{M} + \text{Na}]^+$ , 204.1 (25), 502.3  $[\text{18}, \text{M} + \text{H}]^+$ , 356.2 (18); ESI<sup>-</sup>-MS,  $m/z$  500.2  $[\text{100}, \text{M} - \text{H}]^-$ , 1001.5  $[\text{18}, 2 \text{M} - \text{H}]^-$ , 336.2 (12), 276.0 (5), 202.1 (3). GlcNAc-Rha-Rbo-9TMS: MS (EI)  $m/z$  (%) 73 (100), 204 (97), 173 (85), 217 (73), 330 (59), 147 (46), 103 (33), 420 (30), 363 (30), 273 (21), 451 (10), 240 (8), 115 (6), 492 (2) (Figure 3); RI on DB-5, 3515.

**Rha-Rbo.**  $\text{C}_{11}\text{H}_{22}\text{O}_9$ ; HR-ToF-MS (ESI+)  $m/z$  321.1150 ( $[\text{M} + \text{Na}]^+$ , measured);  $m/z$  321.1156 ( $[\text{M} + \text{Na}]^+$ , calculated for  $\text{NaC}_{11}\text{H}_{22}\text{O}_9$ ; ESI<sup>+</sup>-MS,  $m/z$  321.1  $[\text{100}, \text{M} + \text{Na}]^+$ , 299.1  $[\text{16}, \text{M} + \text{H}]^+$ , 175 (8); ESI<sup>-</sup>-MS,  $m/z$  298.1  $[\text{100}, \text{M} - \text{H}]^-$ , 595.2  $[\text{12}, 2 \text{M} - \text{H}]^-$ . Rha-Rbo-7TMS: MS (EI)  $m/z$  (%) 204 (100), 73 (96), 217 (49), 147 (47), 129 (39), 103 (21), 243 (16), 363 (14), 273 (12), 333 (10), 423 (5), 115 (5) (Figure 3); RI on DB-5, 2487.

**GlcNAc-Rbo.**  $\text{C}_{13}\text{H}_{25}\text{NO}_{10}$ ; HR-ToF-MS (ESI+)  $m/z$  378.1376 ( $[\text{M} + \text{Na}]^+$ , measured);  $m/z$  378.1370 ( $[\text{M} + \text{Na}]^+$ , calculated for  $\text{NaC}_{13}\text{H}_{25}\text{NO}_{10}$ ; ESI<sup>+</sup>-MS,  $m/z$  378.1  $[\text{100}, \text{M} + \text{Na}]^+$ , 356.2  $[\text{18}, \text{M} + \text{H}]^+$ , 226.1 (10); ESI<sup>-</sup>-MS,  $m/z$  354.1  $[\text{100}, \text{M} - \text{H}]^-$ , 707.1  $[\text{18}, 2 \text{M} - \text{H}]^-$ . GlcNAc-Rbo-7TMS: MS (EI)  $m/z$  (%) 73 (100), 173 (80), 217 (58), 330 (50), 147 (45), 129 (40), 103 (29), 246 (19), 420 (14), 271 (7) (Figure 3); RI on DB-5, 2845.

#### Liquid Chromatography-Mass Spectrometry (LC-MS).

LC-MS analysis of the purified WTA monomer of 10403S was performed with an Agilent 1260 series HPLC system (Agilent Technologies Inc., Santa Clara, CA). The system was equipped with an autosampler, a BIN Pump SL binary pump, a TCC SL thermostated column compartment, and a DADSL diode array detector, interfaced to a 6410 triple-quadrupole LC-MS mass selective detector equipped with an API-ESI ionization source. Prior to injection, the sample was dissolved in methanol to a concentration of 1 mg/mL. Chromatographic separations for 10  $\mu\text{L}$  injection volumes were performed using a Gemini column (250  $\times$  4.6 mm i.d.; 5.0  $\mu\text{m}$  particle size) (Phenomenex, Torrance, CA). The column temperature was set at 25  $^\circ\text{C}$  and operated at a 1.0 mL/min flow rate. DI water with 0.1% formic acid (A) and methanol with 0.1% formic acid (B) were employed in the binary mobile phase with a linear gradient of 5–55% over 50 min; 55–90% over 5 min; elution at 90% for 5 min, followed by re-equilibration over 10 min. Data acquisition and analysis were performed using Mass Hunter Workstation Data Acquisition, Qualitative Analysis, and Quantitative Analysis software. LC-MS analysis was performed in both negative and positive ion mode with ionization parameters set at capillary voltage, 3.5 kV; nebulizer pressure, 35 psi; drying gas flow, 13.0 mL/min; drying gas temperature, 350  $^\circ\text{C}$ ; and mass scan range,  $m/z$  300–2000. Quantitative analysis of the sample was performed in negative ion mode with the same ionization parameters as described above.

#### Sample Preparation for GC-FID and GC-MS Analysis.

**Hydrofluoric Acid Hydrolysis.** Hydrofluoric acid hydrolysis of

samples was conducted as described above. 50  $\mu\text{L}$  of 1,3,5-trihydroxybenzene (400  $\mu\text{g}/\text{mL}$  DI  $\text{H}_2\text{O}$ ) was added as an internal standard. Samples (10 mg; each of each strain), including in-process ACP, CWCF, and cWTA polymer (for the streamlining experiment) were subjected to hydrolysis using 200  $\mu\text{L}$  of HF (48–51%) at 0  $^\circ\text{C}$  for 20 h prior to evaporation over NaOH pellets in a chamber under vacuum. Samples were subjected to a vacuum until HF evaporation was complete; the sample was then mixed with 500  $\mu\text{L}$  of ultrapure water, frozen at  $-20$   $^\circ\text{C}$ , lyophilized, and stored at  $-20$   $^\circ\text{C}$  with a desiccant, prior to derivatization and GC-FID and GC-MS analysis.

**Sample Derivatization.** Prior to GC-FID and GC-MS analysis, standards and samples were derivatized similarly to the methods used by Munafo et al.<sup>39</sup> with modifications. Approximately 1 mg of the purified WTA monomer sample for each strain and approximately 1 mg each of the streamlining samples (i.e., ACP, CWCF, and cWTA polymer) were derivatized in Reacti-Vials (Thermo Fisher Scientific Inc., Waltham, MA) at 70  $^\circ\text{C}$  for 1 h using a mixture of 7 parts anhydrous pyridine and 3 parts BSTFA with 1% TMCS for a total volume of 100  $\mu\text{L}$  (Thermo Scientific, Bellefonte, PA). Standards of Rha and Rbo were derivatized similarly, using 1 mg of each with a total volume of 1 mL derivatizing reagents (Figure 2). Samples were then analyzed by GC-FID and GC-MS. For comparison of WTA monomers in each mutant strain, the areas of each WTA monomer were normalized based on the area of Rbo-5TMS in the 10403S sample using the following equation:  $\text{Area}_{\text{normalized}} = (\text{Analyte}_{\text{sample}} \times \text{Rbo-5TMS}_{10403\text{S}}) / \text{Rbo-5TMS}_{\text{sample}}$ .

**Gas Chromatography-Flame Ionization Detection (GC-FID).** GC-FID (6890 Series; Agilent Technologies, Santa Clara, CA) analysis was conducted similarly to the methods used by Munafo et al.<sup>39</sup> with some modifications. GC-FID was performed by manual injection (Hamilton Company, Bonaduz, Switzerland) with 1  $\mu\text{L}$  of the derivatized sample and a split ratio of 1:10. The inlet temperature was 250  $^\circ\text{C}$ . Helium was used as the carrier gas at a flow rate of 1.5 mL/min. The oven was set to an initial temperature of 80  $^\circ\text{C}$  (held for 1 min) with ramp of 6  $^\circ\text{C}/\text{min}$  to 300  $^\circ\text{C}$  and held for 15 min. The total run time was 53.67 min. The column used was an HP-5 with capillary size 30.0 m  $\times$  0.32 mm  $\times$  0.25  $\mu\text{m}$  (Agilent). The detector temperature was 250  $^\circ\text{C}$ . Data was analyzed using GC ChemStation Rev. A 10.02 [1757] software (Agilent). Linear RIs were determined for each analyte using the retention times of the analyte and *n*-alkanes (C9–C40) by linear interpolation.

**Gas Chromatography–Mass Spectrometry (GC–MS).** GC–MS was performed on an Agilent 6890 series gas chromatograph (Agilent Technologies, Santa Clara, CA, USA) coupled to an Agilent 5973 mass spectrometer detector. The capillary column used for chromatographic separation was a fused silica DB-5 column (30 m  $\times$  0.25 mm  $\times$  0.25  $\mu\text{m}$ ; Agilent). A 1  $\mu\text{L}$  split/spitless injection (1:1 split) was made by an autosampler using a 10  $\mu\text{L}$  syringe. The inlet temperature was 250  $^\circ\text{C}$ . Helium was used as a carrier gas with a constant flow of 1.5 mL/min. The oven temperature was initially held at 80  $^\circ\text{C}$  for 1 min followed by an increase in temperature at a rate of 6  $^\circ\text{C}/\text{min}$  until the oven temperature reached 280  $^\circ\text{C}$  and held at this temperature for 90 min. The mass spectrometer detector was coupled to the GC via a transfer line heated at 280  $^\circ\text{C}$  and operated in electron ionization (EI)

mode at 70 eV. The total run time was 124.338 min. The detector scan range was set to  $m/z$  50–800.

**High Resolution Electrospray Ionization-Time-of-Flight Mass Spectrometry (HRESI-TOFMS).** High resolution mass spectra were recorded on a Bruker BioTOF II ESI under the following conditions: source temperature, 150  $^\circ\text{C}$ ; acceleration voltage, 8500; mass resolution, 10 000 fwhm; scan range,  $m/z$  100–1400; drying gas,  $\text{N}_2$ .

## ■ ASSOCIATED CONTENT

### Supporting Information

The Supporting Information is available free of charge at <https://pubs.acs.org/doi/10.1021/acsomega.1c07403>.

GC-FID trace of GlcNAc-Rbo-7TMS, GC-FID trace of Rha-Rbo-7TMS, and GC-FID trace of GlcNAc-Rha-Rbo-9TMS (PDF)

## ■ AUTHOR INFORMATION

### Corresponding Authors

John P. Munafo, Jr. – Department of Food Science, University of Tennessee, Knoxville, Tennessee 37996, United States;

orcid.org/0000-0003-4702-2955; Phone: 865-974-7247; Email: [jmunaf@utk.edu](mailto:jmunaf@utk.edu)

Thomas G. Denes – Department of Food Science, University of Tennessee, Knoxville, Tennessee 37996, United States; Phone: 865-974-7425; Email: [tdenes@utk.edu](mailto:tdenes@utk.edu)

### Authors

Danielle M. Trudelle – Department of Food Science, University of Tennessee, Knoxville, Tennessee 37996, United States

Daniel W. Bryan – Department of Food Science, University of Tennessee, Knoxville, Tennessee 37996, United States

Shahla Ray – Department of Food Science, University of Tennessee, Knoxville, Tennessee 37996, United States

Complete contact information is available at:

<https://pubs.acs.org/10.1021/acsomega.1c07403>

### Notes

The authors declare no competing financial interest.

## ■ ACKNOWLEDGMENTS

This work was supported by the USDA National Institute of Food and Agriculture Hatch Projects #1015002 and #1016031, and startup funds provided from the University of Tennessee Institute of Agriculture to J.P.M. and T.G.D.

## ■ ABBREVIATIONS

ESI, electrospray ionization; GC-FID, gas chromatography-flame ionization detection; GC-MS, gas chromatography-mass spectrometry; GlcNAc, *N*-acetylglucosamine; HRESI-TOFMS, high resolution electrospray ionization-time-of-flight mass spectrometry; LC-MS, liquid chromatography-mass spectrometry; NMR, nuclear magnetic resonance; Rbo, ribitol; Rha, rhamnose; RI, retention index; UPLC, ultraperformance liquid chromatography; WTA, wall teichoic acid

## ■ REFERENCES

(1) Vázquez-Boland, J. A.; Kuhn, M.; Berche, P.; Chakraborty, T.; Domínguez-Bernal, G.; Goebel, W.; González-Zorn, B.; Wehland, J.; Kreft, J. *Listeria Pathogenesis and Molecular Virulence Determinants*. *Clin. Microbiol. Rev.* **2001**, *14* (3), 584–640.

- (2) Linnan, M. J.; Mascola, L.; Lou, X. D.; Goulet, V.; May, S.; Salminen, C.; Hird, D. W.; Yonekura, M. L.; Hayes, P.; Weaver, R.; Audurier, A.; Plikaytis, B. D.; Fannin, S. L.; Kleks, A.; Broome, C. V. Epidemic Listeriosis Associated with Mexican-Style Cheese. *N. Engl. J. Med.* **1988**, *319* (13), 823–828.
- (3) McCollum, J. T.; Cronquist, A. B.; Silk, B. J.; Jackson, K. A.; O'Connor, K. A.; Cosgrove, S.; Gossack, J. P.; Parachini, S. S.; Jain, N. S.; Ettestad, P.; Ibraheem, M.; Cantu, V.; Joshi, M.; DuVernoy, T.; Fogg, N. W., Jr; Gorny, J. R.; Mogen, K. M.; Spires, C.; Teitell, P.; Joseph, L. A.; Tarr, C. L.; Imanishi, M.; Neil, K. P.; Tauxe, R. V.; Mahon, B. E. Multistate Outbreak of Listeriosis Associated with Cantaloupe. *N. Engl. J. Med.* **2013**, *369* (10), 944–953.
- (4) Salama, P. J.; Embarek, P. K. B.; Bagaria, J.; Fall, I. S. Learning from Listeria: Safer Food for All. *Lancet* **2018**, *391* (10137), 2305–2306.
- (5) Hoffman, S.; Macculloch, B.; Batz, M. *Economic Burden of Major Foodborne Illnesses Acquired in the United States*; Economic Information Bulletin No. EIB-140; USDA, 2015.
- (6) Scallan, E.; Hoekstra, R. M.; Angulo, F. J.; Tauxe, R. V.; Widdowson, M.-A.; Roy, S. L.; Jones, J. L.; Griffin, P. M. Foodborne Illness Acquired in the United States—Major Pathogens. *Emerg. Infect. Dis.* **2011**, *17* (1), 7–15.
- (7) Silk, B.; Mahon, B.; Griffin, P. M.; Gould, L. H. Vital Signs: Listeria Illnesses, Deaths, and Outbreaks—United States, 2009–2011. *MMWR Morb. Mortal. Wkly. Rep.* **2013**, *62* (22), 448–452.
- (8) Fiedler, F. Biochemistry of the Cell Surface of Listeria Strains: A Locating General View. *Infection* **1988**, *16* (2), S92–7.
- (9) Weidenmaier, C.; Peschel, A. Teichoic Acids and Related Cell-Wall Glycopolymers in Gram-Positive Physiology and Host Interactions. *Nature Reviews Microbiology* **2008**, *6*, 276–287.
- (10) Brown, S.; Santa Maria, J. P., Jr; Walker, S. Wall Teichoic Acids of Gram-Positive Bacteria. *Annu. Rev. Microbiol.* **2013**, *67*, 313–336.
- (11) Reichmann, N. T.; Gründling, A. Location, Synthesis and Function of Glycolipids and Polyglycerolphosphate Lipoteichoic Acid in Gram-Positive Bacteria of the Phylum Firmicutes. *FEMS Microbiol. Lett.* **2011**, *319* (2), 97–105.
- (12) Dell'Era, S.; Buchrieser, C.; Couvé, E.; Schnell, B.; Briens, Y.; Schuppler, M.; Loessner, M. J. Listeria Monocytogenes L-Forms Respond to Cell Wall Deficiency by Modifying Gene Expression and the Mode of Division. *Mol. Microbiol.* **2009**, *73* (2), 306–322.
- (13) Carvalho, F.; Atilano, M. L.; Pombinho, R.; Covas, G.; Gallo, R. L.; Filipe, S. R.; Sousa, S.; Cabanes, D. L-Rhamnosylation of Listeria Monocytogenes Wall Teichoic Acids Promotes Resistance to Antimicrobial Peptides by Delaying Interaction with the Membrane. *PLoS Pathog.* **2015**, *11* (5), No. e1004919.
- (14) Eugster, M. R.; Haug, M. C.; Huwiler, S. G.; Loessner, M. J. The Cell Wall Binding Domain of Listeria Bacteriophage Endolysin PlyP35 Recognizes Terminal GlcNAc Residues in Cell Wall Teichoic Acid. *Mol. Microbiol.* **2011**, *81* (6), 1419–1432.
- (15) Shen, Y.; Boulos, S.; Sumrall, E.; Gerber, B.; Julian-Rodero, A.; Eugster, M. R.; Fieseler, L.; Nyström, L.; Ebert, M.-O.; Loessner, M. J. Structural and Functional Diversity in Listeria Cell Wall Teichoic Acids. *J. Biol. Chem.* **2017**, *292* (43), 17832–17844.
- (16) Orsi, R. H.; den Bakker, H. C.; Wiedmann, M. Listeria Monocytogenes Lineages: Genomics, Evolution, Ecology, and Phenotypic Characteristics. *Int. J. Med. Microbiol.* **2011**, *301* (2), 79–96.
- (17) Cartwright, E. J.; Jackson, K. A.; Johnson, S. D.; Graves, L. M.; Silk, B. J.; Mahon, B. E. Listeriosis Outbreaks and Associated Food Vehicles, United States, 1998–2008. *Emerg. Infect. Dis.* **2013**, *19* (1), 1–9 quiz 184.
- (18) Eugster, M. R.; Morax, L. S.; Hüls, V. J.; Huwiler, S. G.; Leclercq, A.; Lecuit, M.; Loessner, M. J. Bacteriophage Predation Promotes Serovar Diversification in Listeria Monocytogenes. *Mol. Microbiol.* **2015**, *97* (1), 33–46.
- (19) Kamisango, K.; Fujii, H.; Okumura, H.; Saiki, I.; Araki, Y.; Yamamura, Y.; Azuma, I. Structural and Immunochemical Studies of Teichoic Acid of Listeria Monocytogenes. *J. Biochem.* **1983**, *93* (5), 1401–1409.
- (20) García, P.; Rodríguez, L.; Rodríguez, A.; Martínez, B. Food Biopreservation: Promising Strategies Using Bacteriocins, Bacteriophages and Endolysins. *Trends Food Sci. Technol.* **2010**, *21* (8), 373–382.
- (21) Biemann, R.; Habann, M.; Eugster, M. R.; Lurz, R.; Calendar, R.; Klumpp, J.; Loessner, M. J. Receptor Binding Proteins of Listeria Monocytogenes Bacteriophages A118 and P35 Recognize Serovar-Specific Teichoic Acids. *Virology* **2015**, *477*, 110–118.
- (22) Denes, T.; den Bakker, H. C.; Tokman, J. I.; Guldimmann, C.; Wiedmann, M. Selection and Characterization of Phage-Resistant Mutant Strains of Listeria Monocytogenes Reveal Host Genes Linked to Phage Adsorption. *Appl. Environ. Microbiol.* **2015**, *81* (13), 4295–4305.
- (23) Trudelle, D. M.; Bryan, D. W.; Hudson, L. K.; Denes, T. G. Cross-Resistance to Phage Infection in Listeria Monocytogenes Serotype 1/2a Mutants. *Food Microbiology* **2019**, *84*, 103239.
- (24) Song, Y.; Peters, T. L.; Bryan, D. W.; Hudson, L. K.; Denes, T. G. Homburgvirus LP-018 Has a Unique Ability to Infect Phage-Resistant Listeria Monocytogenes. *Viruses* **2019**, *11*, 1166.
- (25) Peters, T. L.; Song, Y.; Bryan, D. W.; Hudson, L. K.; Denes, T. G. Mutant and Recombinant Phages Selected from In Vitro Coevolution Conditions Overcome Phage-Resistant Listeria Monocytogenes. *Appl. Environ. Microbiol.* **2020**, *86* (22). DOI: 10.1128/AEM.02138-20.
- (26) de Melo, A. G.; Levesque, S.; Moineau, S. Phages as Friends and Enemies in Food Processing. *Curr. Opin. Biotechnol.* **2018**, *49*, 185–190.
- (27) Denes, T.; Wiedmann, M. Environmental Responses and Phage Susceptibility in Foodborne Pathogens: Implications for Improving Applications in Food Safety. *Current Opinion in Biotechnology* **2014**, *26*, 45–49.
- (28) Fujii, H.; Kamisango, K.; Nagaoka, M.; Uchikawa, K.; Sekikawa, I.; Yamamoto, K.; Azuma, I. Structural Study on Teichoic Acids of Listeria Monocytogenes Types 4a and 4d. *J. Biochem.* **1985**, *97* (3), 883–891.
- (29) Kaya, S.; Araki, Y.; Ito, E. Characterization of a Novel Linkage Unit between Ribitol Teichoic Acid and Peptidoglycan in Listeria Monocytogenes Cell Walls. *Eur. J. Biochem.* **1985**, *146* (3), 517–522.
- (30) Fiedler, F.; Seger, J.; Schrettenbrunner, A.; Seeliger, H. P. R. The Biochemistry of Murein and Cell Wall Teichoic Acids in the Genus Listeria. *Syst. Appl. Microbiol.* **1984**, *5* (3), 360–376.
- (31) Wendlinger, G.; Loessner, M. J.; Scherer, S. Bacteriophage Receptors on Listeria Monocytogenes Cells Are the N-Acetylglucosamine and Rhamnose Substituents of Teichoic Acids or the Peptidoglycan Itself. *Microbiology* **1996**, *142*, 985–992.
- (32) Uchikawa, K.-I.; Sekiawa, I.; Azuma, I. Structural Studies on Teichoic Acids in Cell Walls of Several Serotypes of Listeria Monocytogenes. *Journal of Biochemistry* **1986**, *99*, 315–327.
- (33) Eugster, M. R.; Loessner, M. J. Rapid Analysis of Listeria Monocytogenes Cell Wall Teichoic Acid Carbohydrates by ESI-MS/MS. *PLoS One* **2011**, *6* (6), No. e21500.
- (34) Giraud, M. F.; Leonard, G. A.; Field, R. A.; Berling, C.; Naismith, J. H. RmlC, the Third Enzyme of DTDP-L-Rhamnose Pathway, Is a New Class of Epimerase. *Nat. Struct. Biol.* **2000**, *7* (5), 398–402.
- (35) Carvalho, F.; Sousa, S.; Cabanes, D. L-Rhamnosylation of Wall Teichoic Acids Promotes Efficient Surface Association of Listeria Monocytogenes Virulence Factors InlB and Ami through Interaction with GW Domains. *Environ. Microbiol.* **2018**, *20* (11), 3941–3951.
- (36) Zhu, X.; Liu, D.; Singh, A. K.; Droli, R.; Bai, X.; Tenguria, S.; Bhunia, A. K. Tunicamycin Mediated Inhibition of Wall Teichoic Acid Affects Staphylococcus Aureus and Listeria Monocytogenes Cell Morphology, Biofilm Formation and Virulence. *Front. Microbiol.* **2018**. DOI: 10.3389/fmicb.2018.01352.
- (37) Sumrall, E. T.; Shen, Y.; Keller, A. P.; Rismondo, J.; Pavlou, M.; Eugster, M. R.; Boulos, S.; Disson, O.; Thouvenot, P.; Kilcher, S.; Wollscheid, B.; Cabanes, D.; Lecuit, M.; Gründling, A.; Loessner, M. J. Phage Resistance at the Cost of Virulence: Listeria Monocytogenes

Serovar 4b Requires Galactosylated Teichoic Acids for InIB-Mediated Invasion. *PLoS Pathog.* **2019**, *15* (10), No. e1008032.

(38) Sumrall, E. T.; Röhrig, C.; Hupfeld, M.; Selvakumar, L.; Du, J.; Dunne, M.; Schmelcher, M.; Shen, Y.; Loessner, M. J. Glycotyping and Specific Separation of *Listeria Monocytogenes* with a Novel Bacteriophage Protein Tool Kit. *Appl. Environ. Microbiol.* **2020**, *86* (13). DOI: [10.1128/AEM.00612-20](https://doi.org/10.1128/AEM.00612-20).

(39) Munafo, J. P., Jr; Ramanathan, A.; Jimenez, L. S.; Gianfagna, T. J. Isolation and Structural Determination of Steroidal Glycosides from the Bulbs of Easter Lily (*Lilium Longiflorum* Thunb.). *J. Agric. Food Chem.* **2010**, *58* (15), 8806–8813.